06

Effect of strain aging of carbon steel after dynamic loading

© G.S. Nagicheva,[1] A.V. Nokhrin,[1] N.V. Melekhin,[1] N.N. Berendeev,[1] A.M. Bragov,[1] V.V. Balandin,[1] A.N. Sysoev,[1] M.Yu. Gryaznov,[1] V.V. Gundorin,[2] S.A. Kurepin,[2] A.S. Smirnov[2]

[1] Lobachevsky University of Nizhny Novgorod
603022 Nizhny Novgorod, Russia
[2] V.V. Bakhirev Institute of Mechanical Engineering,
606002 Dzerzhinsk, Nizhny Novgorod region, Russia
e-mail: nagichevags@gmail.com

Received July 21, 2023
Revised September 23, 2023
Accepted October 21, 2023

The tendency of the samples of the carbon steel U8 after (i) dynamic compression, which has been executed by throwing a steel flat striker by means of a gas gun, (ii) explosive processing of a cylindrical workpiece and quasistatic compression to strain aging has been investigated. The Finite Element Method with the application of the Johnson–Cook model has been utilized to estimate the strain after dynamic loading. The scale of strain aging has been determined from the change in the microhardness (ΔHv) of the steel after annealing in the temperature range of 150–500°C, likewise from the change in the highest of the Snoek–Koester peak on the temperature curve of internal friction. It has been demonstrated that the maximum scale of strain aging is observed after dynamic compression.

Keywords: carbon steel, pearlite, strain aging, dynamic loading, Johnson–Cook model.

DOI: 10.61011/JTF.2024.01.56908.186-23

Introduction

The effect of strain aging (SA) increases the hardness of steel during annealing after deformation [1]. The SA effect often negatively affects the steel toughness, but it can provide an optimal combination of strength, hardness and ductility of steel in case of optimization of thermal deformation treatment conditions [2]. Currently, there is a well-developed theory of SA of steels, which focuses on the interaction of mobile carbon and nitrogen atoms with lattice dislocations [3]. For example, carbon and nitrogen atoms with high diffusion mobility in the iron crystal lattice, even at low temperatures, block the movement of dislocations in the Cottrell model and so contribute to an increase of the steel hardness [4].

Carbon steels are widely used in mechanical engineering for the manufacturing of highly critical products. Such steels have a lamellar perlite structure in the normalized state, which is a eutectoid mixture of brittle plates of cementite Fe_3C and ductile ferrite [5]. The plastic flow and failure resistance of the Fe–Fe_3C composite determines many of the performance characteristics of products made from these steels [6]. It should be noted that long-range internal stress fields formed by lattice dislocations result in the failure of plates Fe_3C and an increase of the concentration of carbon atoms in the ferrite lattice [7,8]. As a result, the scale of the SA effect in carbon steels with a lamellar perlite structure is closely related to the density and distribution of dislocations.

It should be noted that the mechanisms of high-speed deformation of steels with a lamellar perlite structure is actively studied [9]. Up to the present time there is no unified physical theory of the process of dynamic deformation of Fe–Fe_3C composites, in which the thickness of ferrite and cementite plates can vary from hundreds of nanometers to few microns [10,11].

The purpose of this work is to study the SA susceptibility of U8 steel after various types of deformation. Special attention is paid to the study of SA after high-speed loading of carbon steel. Low-temperature embrittlement of highly critical structural elements made of U8 steel after their dynamic loading is an undesirable process and can results in the degradation of their performance. Therefore, studying the effect of steel SA after dynamic loading has a great practical relevance.

1. Experimental procedure

The object of the study was U8 steel in a normalized state. The samples were examined in their initial state, after quasi-static and dynamic compression to a given strain degree, as well as after explosive treatment.

Quasi-static compression of cylindrical samples with Ø 12.1 mm and initial height of $h = 11.9$ mm was carried out using a hydraulic press EU-40 (40 tf). The samples were compressed at room temperature to the strain degree of deformation $\varepsilon = 5.4$, 6.9, 15.1 and 34.7%. The average loading rate was 1 mm/s; the average deformation rate of the steel sample was $\sim 0.08\,s^{-1}$.

The dynamic compression technique was implemented using 20 mm PG-20 gas gun, which allows throwing samples at speeds up to 800 m/s (using compressed

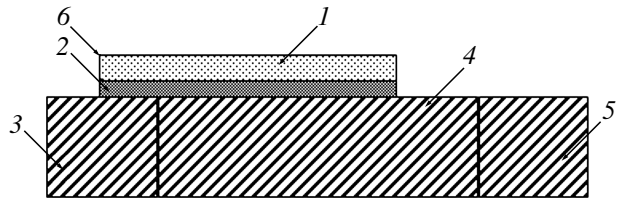

Figure 1. Test circuit: *1* — explosive (Ex), *2* — substrate, *3* — attachment cylinder, *4* — sample, *5* — flip-off cylinder, *6* — place of initiation of explosives.

helium) [12,13]. A flat steel impactor with a diameter of 19.8 mm and a height of 1.5mm was used for impact loading. It struck the test sample of steel U8 with a diameter of 14 mm and a length of 6 mm, located in a high-strength steel cage with a cross section of 36×5.5mm with a hole under the sample. The difference between the length of the sample and the thickness of the steel cage regulated the strain degree of the sample. The average degree of strain was 5%. The amplitude of the compression wave depended on the velocity of the impactor (209−654 m/s).

The explosive loading technique was implemented at the site of JSC „GosNIImash named after V.V. Bakhirev". Fig. 1 shows the scheme of explosive loading of a cylindrical billet with a diameter of 128 mm made of steel U8. The clockwork initiation site was located on a attached wheel. „Spallation" cylinder was attached to the end surface for reducing the impact of the unloading waves. The test modes are listed in Table 1.

Cylindrical samples with a diameter of 19.8mm and a height of 11 mm were cut out of the deformed workpiece on an electrical discharge machine. The samples were cut from the area adjacent to the substrate with an explosive substance (detonation zone), the central area of the cylindrical workpiece and the zone opposite to the area adjacent to the explosive substance (shock wave reflection area). Similar samples were cut from a non-deformed billet for comparative studies. TG4 ($v = 4$ km/s) was used as an explosive substance.

The steel microstructure was studied using Leica DM IRM metallurgical microscope and Jeol JSM-6490 scanning electron microscope. HVS-1000 hardness tester was used for measuring the hardness (Hv) (load 0.2 kg). Microhardness measurements were carried out in the central zone of the samples. 1-hour annealing of samples was performed in air furnace EKPS-10 for determination of the scale of the SA effect proportional to the magnitude of the change of hardness ΔHv [1]. The temperature dependence of internal friction (Q^{-1}) and the modulus of elasticity (G) was studied using a reverse torsional pendulum, in continuous heating mode at a rate of 4°C/min with a frequency of $\omega = 9$ Hz. Internal friction (IF) was studied using $1.5 \times 1.5 \times 45$ mm samples, cut from billets subjected to quasi-static compression and explosive loading. The IF of samples subjected to dynamic compression was not studied because of the small size of the samples (see above), which did not allow the fabrication of standard-sized samples. The IF method which studies the restructuring of the crystal structure of a material under heating or under the application of periodic mechanical stresses, is one of the classical methods for studying the alloy aging processes [14–16]. The IF method is based on the assumption that it is possible to stimulate the movement of dopant atoms in the crystal lattice by applying an external and periodically varying mechanical stress [14–16]. As is known, the frequency and/or temperature dependences of the relaxation IF have the form of a curve with a maximum, the position of which corresponds to the resonance rule $\omega\tau = 1$, where τ is a characteristic relaxation time depending on temperature in accordance with the Arrhenius equation. The temperature and/or frequency of oscillations at which a peak IF is observed depend on the type of dopant atom and the mechanism of their transition in the crystal lattice [14–16]. The IF peak height is proportional to the concentration of the dopant atoms. Snoek relaxation peak is observed on dependences $Q^{-1}(T)$ in steel at temperatures close to room temperature, which is associated with the diffusive movement of dopant atoms (usually carbon or nitrogen) in the ferrite lattice [14,16]. The Snoek−Koster peak is observed at elevated temperatures with the height proportional to the concentration of dopant atoms embedded on the nuclei of lattice dislocations. Therefore, it is possible to judge the nature of the change of the concentration of carbon dopant atoms in the ferrite lattice and on the nuclei of lattice dislocations, respectively, by determining the height of the Snoek peak at $T \sim 60$°C and the height of the Snoek−Koster peak at $T \sim 240$°C based on the dependence $Q^{-1}(T)$ [14,16].

The explosive loading of a steel billet was simulated using the finite element method with the ANSYS Workbench package. The Johnson−Cook plasticity model [17] was used to solve the problem, which takes into account the dependence of the flow stress on the deformation rate and temperature of the material:

$$\sigma = (A + B\bar{\varepsilon}^{p^n})(1 + C\ln\dot{\varepsilon}^*)\left(1 - (T^*)^m\right),$$

$$T^* = (T - T_0)/(T_m - T_0). \qquad (1)$$

Here $\bar{\varepsilon}^p$ — effective plastic deformation; $\dot{\varepsilon}^* = \dot{\bar{\varepsilon}}^p/\dot{\varepsilon}_0$ — effective plastic deformation rate; $\dot{\varepsilon}_0 = 1\,\mathrm{s}^{-1}$; T_0, T and T_m — ambient temperature, the effective temperature inside the material at a given time and the melting point of the material, respectively. The equation (1) contains five constants which are determined empirically: A — static yield strength, B –strain hardening modulus, n — strain hardening coefficient, C — a coefficient that takes into account the impact of the rate of strain, m — a numerical coefficient that takes into account the impact of temperature on the steel strength. A series of dynamic tests of steel samples U8 was carried out using the Taylor test setup to determine the constants of steel U8 in model (1) [18]. The test results are provided in the Appendix. Numerical values of constants for steel U8 in the Johnson−Cook model were

Table 1. Modes of explosive loading of a cylindrical billet made of steel U8

Mode No	Substrate Filler	Particle Size, μm	Filler content, %	δ, mm	ρ substrates, g/cm^3	h, mm
1	–	–	–	–	–	6
2	Chalk MTD-2	–	60	2	1.9	6
3	SiO_2	30–80	75	2	1.78	6
4	80% Outline-C+20% microspheres	–	60	2	1.46	6
5	Chalk MTD-2	30–80	80	4	1.32	6

Note. δ — thickness of the substrate, h — thickness of the explosive layer.

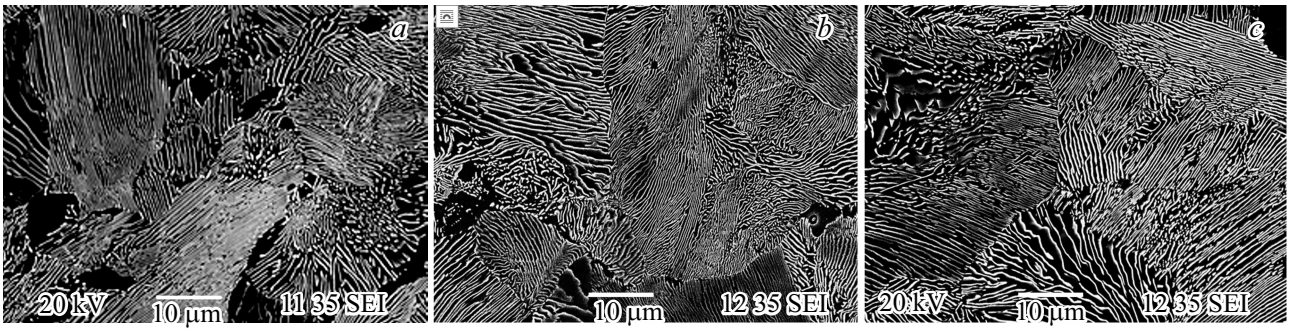

Figure 2. Structure of steel U8: a — initial state; b — compression by 15.1%; c — compression by 34.7%. SEM.

determined based on the analysis of test results using the ANSYS Workbench package: $A = 378$ MPa, $B = 664$ MPa, $n = 0.2$, $C = 0.07$, $m = 1.6$.

2. Experimental results and discussion

2.1. Quasi-static compression

Steel U8 has a microstructure coarse-lamellar perlite with different dispersion of cementite plates in the initial state (Fig. 2, a). Studies of samples after quasi-static compression showed that there are no noticeable changes of the microstructure of steel U8; fragmentation of cementite plates was not detected (Fig. 2, b, c). The hardness of steel U8 in the initial state is $Hv = 2740 \pm 60$ MPa. The quasi-static compression of steel U8 to the strain degree of 34.7% results in a slight increase of Hv to 2970 ± 100 MPa. Therefore, quasi-static strain does not significantly affect the hardness of steel U8 as the average increment in hardness of steel U8 after deformation to 34.7% is ~ 240 MPa.

Fig. 3, a shows the dependence of microhardness on the temperature of 1-hour annealing of steel subjected to quasi-static compression. Fig. 3, a shows that the hardness of the steel in its initial state monotonously decreases from ~ 2730 to ~ 2530 MPa with an increase of the annealing temperature to 500°C ; there is no SA effect. The dependence $Hv(T)$ for deformed steel U8 has a two-stage character with a maximum. The scale of the increase of hardness in case of annealing (ΔHv) depends on the degree of preliminary strain. The maximum hardness increment after deformation 5.4, 6.9, 15.1, 34.7% and 1-hour annealing was $\Delta Hv \sim 155$, 165, 260 and 300 MPa, respectively (Fig. 3, a). The results obtained correspond well to the SA theory [1] — the higher the degree of strain, the higher the density of defects in the steel structure and, consequently, the larger the scale of SA due to the formation of Cottrell atmospheres around lattice dislocations.

Fig. 3, b shows the results of studies of the temperature dependences of internal friction (Q^{-1}) and shear modulus (G) for steel U8 in various structural states. The dependences $Q^{-1}(T)$ and $G(T)$ for steel U8 in the initial state are usually monotonous (Fig. 3, b): a monotonous increase of Q^{-1} and monotonous decrease of G is observed with an increase of temperature.

Strain up to $\varepsilon = 13\%$ results in an increase of IF from $0.52 \cdot 10^{-3}$ to $1.2 \cdot 10^{-3}$ at room temperature (Fig. 3, b). The Snoek peak is clearly visible on the IF temperature dependence for deformed steel (peak height $\Delta Q^{-1} \sim 1.3 \cdot 10^{-3}$) at $T \sim 50$°C as well as the Snoek–Koster peak with maximum ($\Delta Q^{-1} \sim 1.45 \cdot 10^{-3}$) corresponding to $T \sim 270$°C (fig. 3, b). The annealing of deformed steel at temperature of 250°C (1 h) results in a decrease of IF at room temperature to $0.63 \cdot 10^{-3}$, the disappearance of the Snoek peak and a reduction of the height of the Snoek–Koster peak to $\Delta Q^{-1} \sim 1.3 \cdot 10^{-3}$ (Fig. 3, b). The obtained result indicates that the dislocation density increases during compression which is accompanied by an increase of IF at room temperature, and the concentration of carbon atoms increases in the ferrite lattice and on the nuclei of lattice dislocations. Annealing 250°C(1 h) results

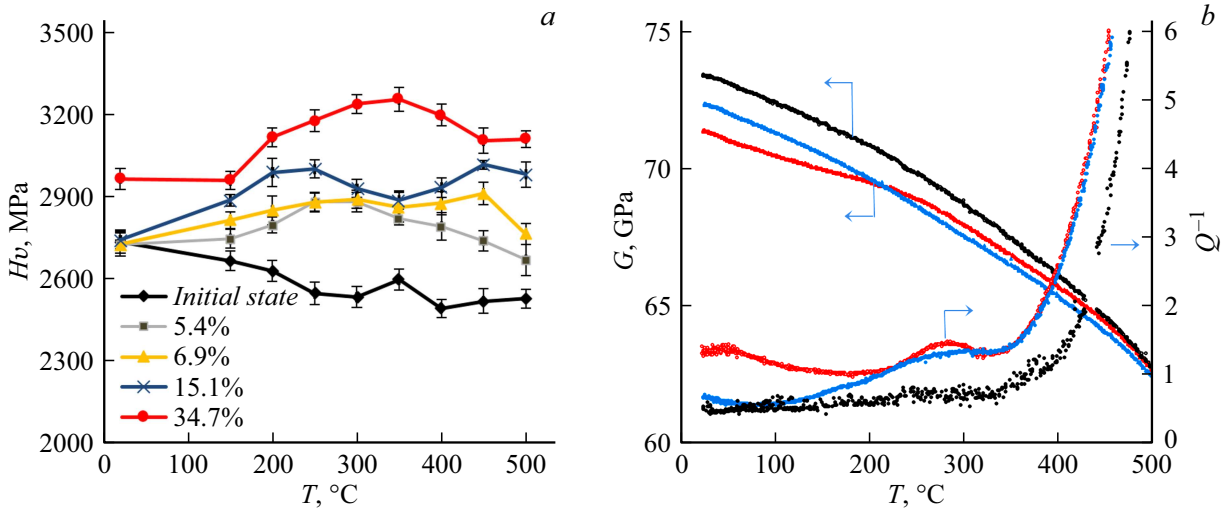

Figure 3. The results of the study of samples of steel U8 after quasi-static compression: *a* — dependence of hardness on the temperature of 1-hour annealing; *b* — temperature dependence IF and modulus of elasticity of steel in the initial state (black markers) subjected to quasi-static compression ($\varepsilon = 13\%$) (red markers) and annealing at 250°C (blue markers).

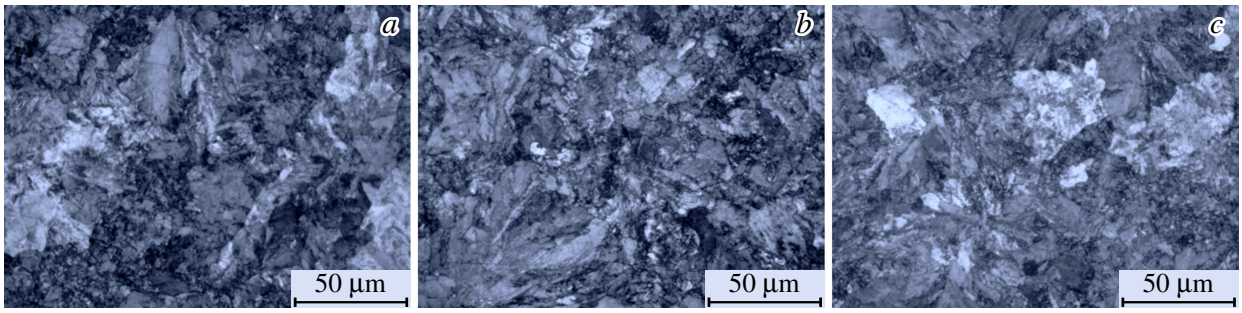

Figure 4. Microstructure of U8 steel after deformation at different rates: *a* — without deformation, *b* — 209 m/s, *c* — 261 m/s. Metallography.

in the diffusion of carbon atoms from the lattice to the dislocation nuclei and, probably, to the formation of particles of cementite Fe_3C in the volume of ferrite grains [19].

2.2. Dynamic compression

Fig. 4 shows the structure of steel U8 after treatment at different impact rates. There were no significant differences in the microstructure of steel after loading with different impact rates. Fragmentation of cementite plates is insignificant. An increase of the loading rate to 261 m/s results in a slight increase of Hv samples to 4130 MPa (Table 2). The average hardness of the sample, deformed at a rate of 654 m/s, is 4150 MPa.

Fig. 5 shows the dependence $Hv(T)$ for steel U8 after dynamic compression. Analysis of the results shows that annealing at 300°C results in $\Delta Hv \approx 300$ MPa increase of the hardness of steel that was pre-loaded at a rate of 291 m/s. Therefore, the scale of SA in steel subjected to dynamic compression to the degree of strain $\sim 5\%$ turns out to be ~ 2 times larger than in the case of quasi-static compression to the same degree of strain. The increase of the rate to 654 m/s and annealing at 200–300°C (1 h) results in an increase of the hardness of the central part of the sample to ~ 4300 MPa.

It should be noted based on the comparison of Fig. 5 and 3, *a* that the maximum hardness for steel U8 after dynamic compression (impact) was observed at a lower annealing temperature than in the case of samples subjected to quasi-static compression. The maximum increase of hardness in case of SA is observed in the material of the central part of the deformed sample (Table 2).

Two consecutive loadings of one sample at a rate of 300 m/s do not result in any increase of the hardness compared with a single loading at a rate of 291 m/s. Table 2 shows that the hardness of the samples coincide within the measurement error. The average hardness increment as a result of SA is ~ 350 MPa, which slightly exceeds the scale of SA in case of annealing of steel subjected to single loading at a rate of 291 m/s (~ 300 MPa).

Table 2. Hardness of samples of steel U8 after dynamic compression

Impact velocity, m/s	0 (initial state)	209	235	261	291	654	300 + 300
Hv, MPa	3800 ± 200	3800 ± 200	4200 ± 100	4100 ± 200	3900 ± 200	4150 ± 50	3900 ± 200

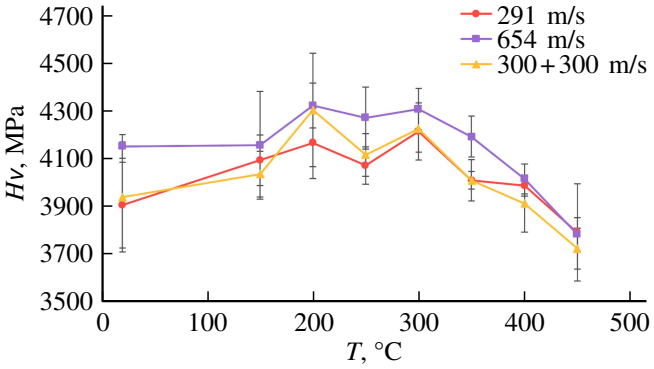

Figure 5. Dependence of hardness on the temperature of 1-hour annealing of steel U8 subjected to dynamic compression at different rates.

2.3. Explosion treatment

Steel U8 after explosion treatment has a coarse-lamellar pearlite microstructure (Fig. 6, *a*) with single regions of spheroidized perlite. The average hardness of steel U8 in the initial state was ∼ 2100 MPa. The hardness of areas with a lamellar perlite structure is ∼ 2500 MPa, the spheroidized perlite has a lower hardness (∼ 1900−2000 MPa).

There are chaotically directed sharp cracks in samples subjected to explosive hardening in mode №1 (loading without a substrate, (Table. 1)), (Fig. 6, *b*); the hardness of steel practically does not change within the measurement error. There are no cracks in case of explosion treatment using the setup with a substrate (modes № 2−5, Table. №1), (Fig. 6, *c*). Explosive treatment did not result in a change of the ratio of the volume fractions of lamellar and spheroidized perlite in the steel structure (within the limits of measurement error ±10 vol.%).

The explosion treatment is accompanied by a slight increase of hardness in the areas of lamellar and spheroidized perlite to ∼ 2700 and ∼ 2100 MPa, respectively. The maximum hardness of steel U8 (∼ 2150 MPa in mode №4) was observed on the surface of the steel billet in the area immediately adjacent to the explosive attachment point, i.e. in the zone of the greatest impact of the shock wave.

Fig. 7, *a* shows the dependencies $Hv(T)$ for steel U8 subjected to explosive loading in various modes. The samples for studies are cut from the central part of the steel billet. It can be seen that Hv does not noticeably increase during annealing and the SA scale ranges from ∼ 20 (modes №1, 5) to ∼ 80 MPa (modes №3, 4). Fig. 7, *a* shows that the spread of „properties from sample to sample“ turns out to be greater than the possible scale of increase of Hv in case of annealing. Thus, the scale of the DC effect in the case of explosive hardening is small and does not exceed the natural spread of mechanical properties.

The explosion results in an increase of Q^{-1} of steel U8 at room temperature from $0.52 \cdot 10^{-3}$ to $0.82 \cdot 10^{-3}$. Fig. 7, *b* shows that the Snoek−Koster peak with a rather small height ($\Delta Q^{-1} \sim 0.80 \cdot 10^{-3}$) is observed on the IF temperature dependence at ∼ 275°C. There is no Snoek peak on the dependence $Q^{-1}(T)$ of explosion-treated steel U8. The result obtained indicates that, although the concentration of carbon atoms on the nuclei of lattice dislocations increases during explosive treatment, their concentration is low. This conclusion is in good agreement with the results of studies of changes of hardness Fig. 7, *a* shows that there is no increase of hardness characteristic of the effect of SA in case of the annealing of steel U8 subjected to explosion treatment [1].

3. Discussion

Analysis of the results shows that quasi-static compression does not significantly change the microstructure of steel U8. The cementite plates are not subjected to any additional fragmentation compared to the initial state. At the same time, it is obvious that steel structure changes at the atomic level in case of compression. The compression results in an increase of the density of dislocations and the concentration of carbon atoms in the ferrite crystal lattice (α-Fe), which act as point barriers for sliding dislocations in case of heating. This is indirectly evidenced by an increase of the hardness of deformed steel in case of annealing (Fig. 3, *a*), which is attributable to the formation of the Cottrell atmospheres around the nuclei of lattice dislocations [4]. It can be assumed in accordance with [19] that the increased concentration of carbon atoms was formed because of the partial destruction of cementite plates in the field of long-range stresses of lattice dislocations. It should be noted that the hardness increment in case of SA (ΔHv) increased with an increase of the strain degree of steel U8. Consequently, the SA effect is sensitive to the degree of pre-strain, which is well consistent with the known results provided in [20].

Dynamic loading has a significant effect on the hardness of steel U8 as the increase of the impact velocity resulted in an increase of dislocation density and, as a result, in an increase of Hv of the steel. It is interesting to note that the scale of hardness increase of case of annealing of steel subjected to dynamic loading before annealing turns out to be noticeably larger than the scale of SA after quasi-static compression (Fig. 3). In particular, as already mentioned above, the value of ΔHv of steel after dynamic compression

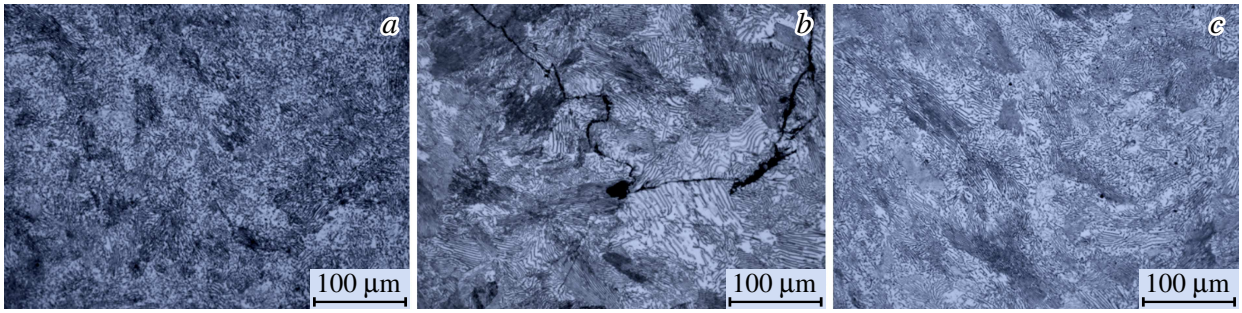

Figure 6. Microstructure of samples cut from the detonation zone: *a* — initial state, *b* — mode №1, *c* — mode №5 (Table 1). Metallography.

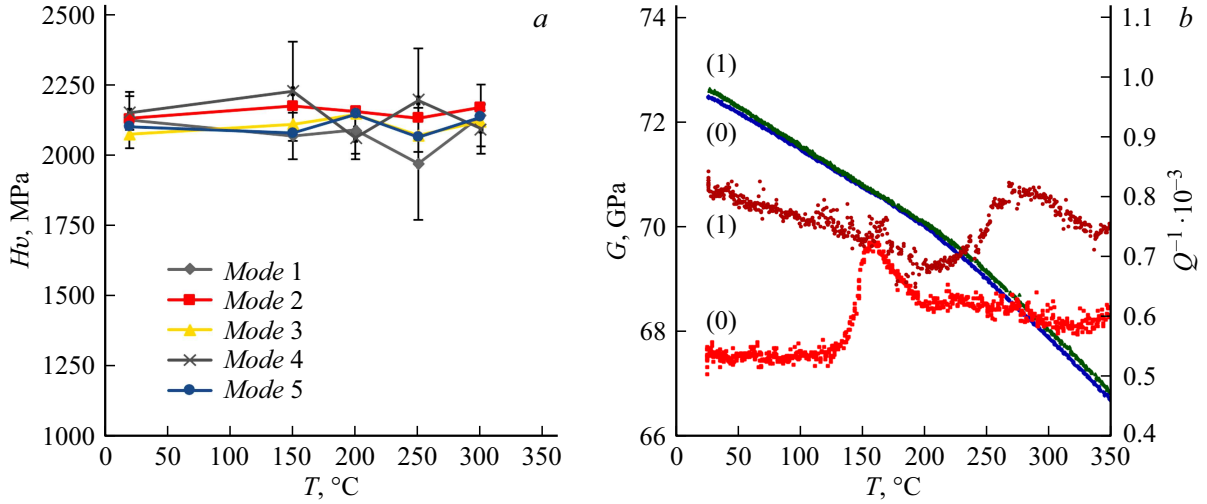

Figure 7. The results of studies of steel U8 subjected to explosive loading: *a* — dependence of hardness on the temperature of 1-hour annealing, *b* — temperature dependence of IF and modulus of elasticity of steel in the initial state (0) and after explosive loading (1)

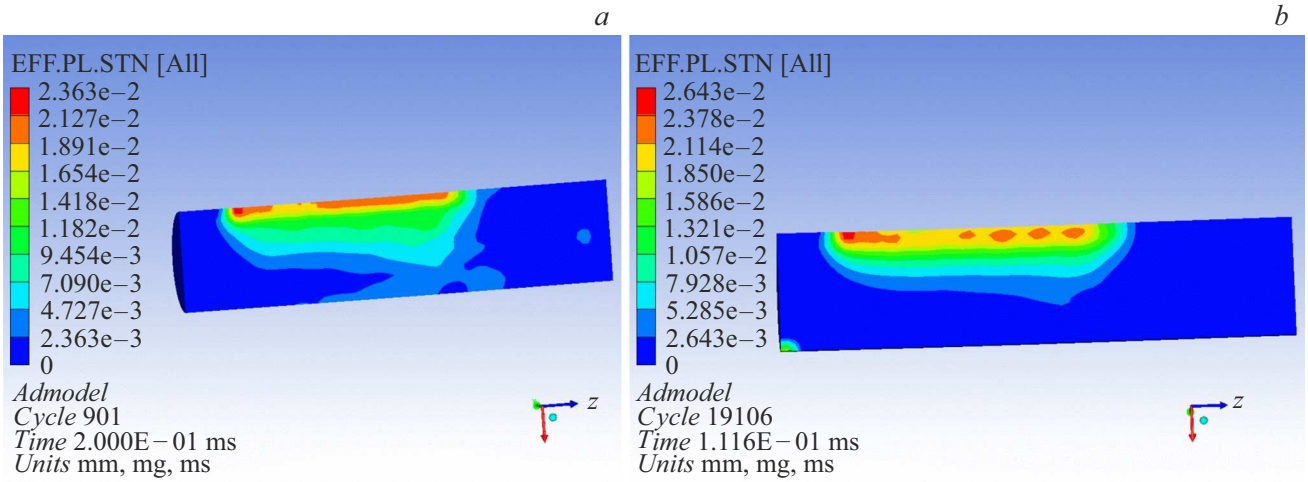

Figure 8. Distribution of plastic deformations in a cylindrical steel billet Y8: *a* — loading without a substrate (mode №1); *b* — loading with a substrate (mode №2).

at ∼ 5% is in 3−3.5 times greater than after quasi-static compression by the same degree of strain. In our opinion, the increased density of dislocations in steel after high-speed loading is the main reason for the observed effect [21]. The second reason may probably be a different nature of the spatial distribution of dislocations compared to the quasi-

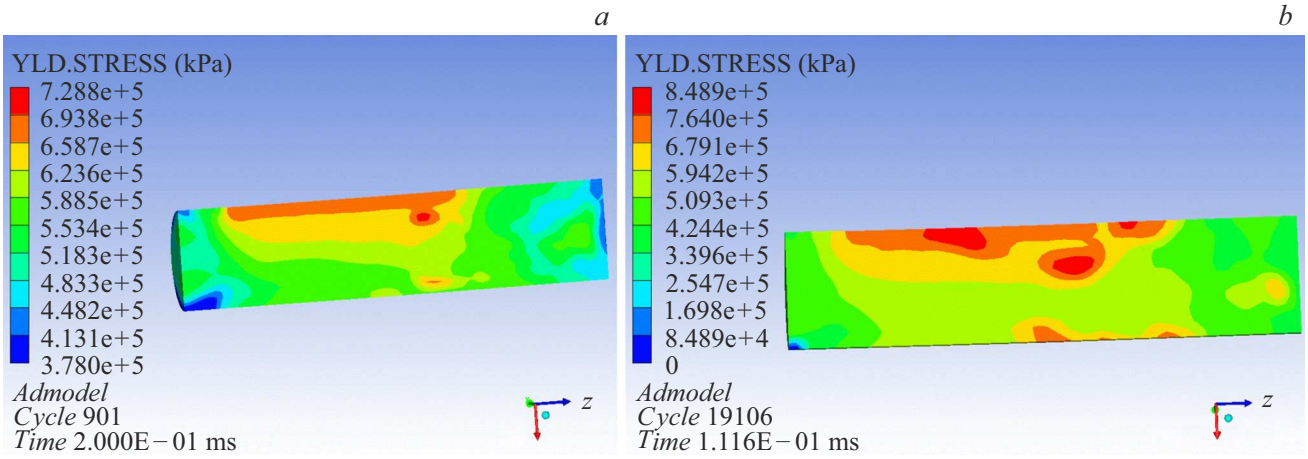

Figure 9. Distribution of calculated values of yield strength in a cylindrical billet made from steel Y8: *a* — mode №1; *b* — mode №2 (Table 1).

static loading of [22], which affects the magnitude of the internal stress field in the material and, as a consequence, the concentration of carbon atoms in the ferrite crystal lattice.

The hardness of steel U8 after explosion treatment practically did not changed compared to the initial state. This indicates that the explosion treatment did not result in any increase of the density of lattice dislocations and the concentration of carbon atoms in the ferrite crystal lattice. This conclusion is confirmed by the results of studies of the SA effect as the explosion treatment did not result in an increase of the hardness of the steel in case of annealing as shown by Fig. 8. One of the most likely reasons for this is, in our opinion, the rapid attenuation of the shock wave in the volume of the steel billet, which prevents from achieving a large degree of plastic deformation and, as a result, it prevents ensuring the operation of dislocation sources in ferrite grains.

Since the correct measurement of the degree of strain in case of an unilateral explosive loading of a cylindrical steel billet is a challenging methodological task, this assumption was verified using computer modeling by the finite element method in the ANSYS Workbench software environment. The analysis of the obtained results showed that the plastic deformation of the steel cylinder is rather heterogeneous. Fig. 8 shows that the degree of local plastic deformation of the steel billet, even in the detonation region, is small ($\sim 2-2.5\%$) and decreases with distance from the location of the explosive substance.

The calculation of the conditional yield strength $\sigma_{0.2}$ using the Johnson–Cook model (see equation (1)) indicates that a very significant hardening of the steel billet should be observed during explosive loading (Fig. 9). Analysis of the results of computer modeling shows that the value of $\sigma_{0.2}$ should increase by more than 2 times in some hardening modes (from ~ 380 to $700-900$ MPa). A noticeable increase of the hardness of the steel billet after explosive loading should be expected because of the well-known correlation between hardness, yield strength and tensile strength of steel [23]. As shown above, the hardness of the workpiece changes very slightly regardless of the explosive loading mode. In our opinion, a more intense heating of the metal during explosive loading compared to the Taylor test is one of the probable reasons for the lack of a significant increase of hardness. The amplitude of the shock wave in the case of explosive loading is known to significantly exceed a similar characteristic in the case of conventional dynamic tests, including Taylor testing [24]. Since the material heating temperature is proportional to the amplitude of the shock wave [25,26], a more significant heating of the metal can be expected in the case of explosive loading as well as a more noticeable decrease of the yield strength of the metal in accordance with equation (1).

Conclusions

The microstructure of steel U8 does not significantly change in case of quasi-static and dynamic strain; fragmentation of cementite plates in perlite is not observed (at degrees of deformation less than 15%).

The largest scale of the SA effect in steel U8 is observed after quasi-static loading, i.e hardness increase (ΔHv) reaches $\Delta Hv = 300$ MPa after compression to a strain degree of 34.7% and 1-hour annealing at 350°C. ΔHv of steel after dynamic compression at $\sim 5\%$ is in $3-3.5$ times greater than after quasi-static compression with the same degree of strain. $200-300$°C is the temperature at which the maximum increase of steel hardness is observed after dynamic compression. The hardness does not significantly increase of the case of explosive treatment; the scale of the SA effect after explosive treatment is also small ($\Delta Hv < 80$ MPa). In our opinion, this is attributable to the rapid attenuation of the blast wave in the steel billet and its heating.

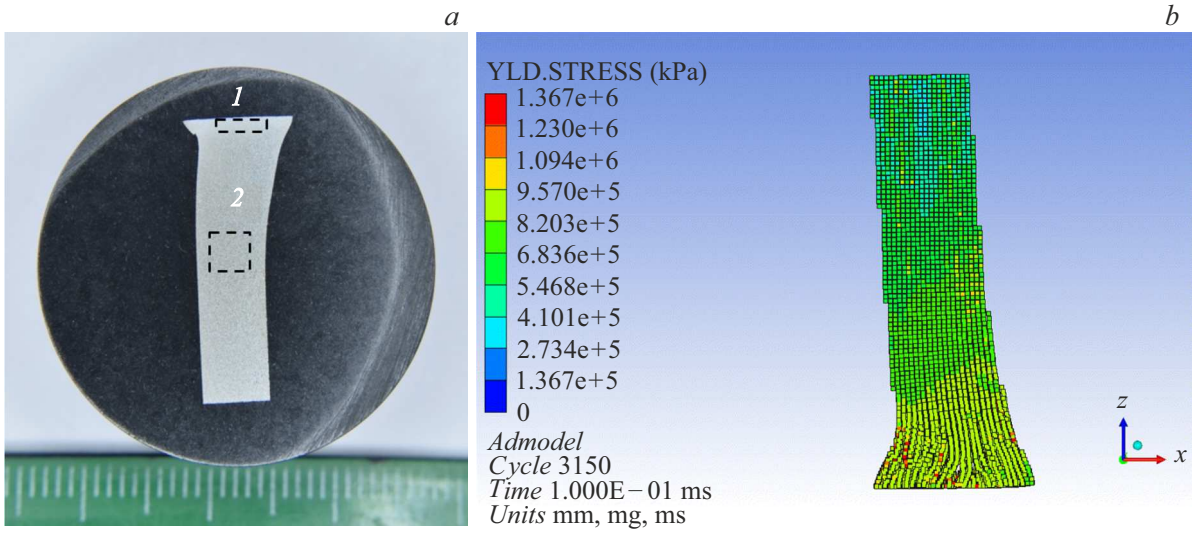

Fig. P1. General view of the sample of steel U8 after testing using the Taylor test method (a) and the results of computer modeling (b). The zones *1* and *2* in Fig. P1, a are indicated by dashed lines.

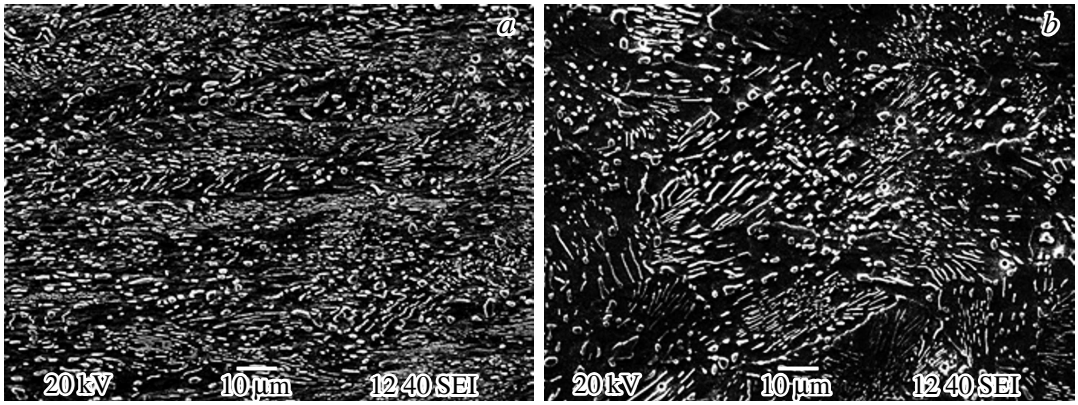

Fig. P2. Microstructure of the sample of steel U8: a — zone №*1*; b — zone №*2*. SEM.

Funding

The study has been funded by the Ministry of Education and Science of Russia (project №FSWR-2023-0037). The microstructure and properties of steels were studied after explosive loading within the framework of the agreement of UNN with JSC GosNIImash (agreement No FT-1910-05).

Conflict of interest

The authors declare that they have no conflict of interest.

Appendix

Study of the strain behavior of steel U8 under dynamic loading using the Taylor test method

Samples of normalized steel U8 with a diameter of 5 mm and a height of $h = 25$ mm were used for testing using the Taylor test setup. The samples were accelerated to a speed of $v = 229$ m/s using 20 mm PG-20 gas gun and collided with a steel barrier. The sample collided with an obstacle at an angle of $\sim 86-87°$. The tests were performed at room temperature. Fig. P1 shows the samples after the test a. The microstructure of steel was studied in the zone of collision of the sample with a steel barrier (zone No 1 in Fig. P1, a) and in a weakly deformed region (zone №2 in fig. P1, a).

The results of the studies of microstructure of the samples are shown in Fig. P2. The microstructure of steel U8 in zone 2 does not significantly changes after the impact. The microstructure of the deformed zone is characterized by the presence of strain localization lines, where intense fragmentation of cementite plates and their orientation along the deformation axis are observed. The grains of spheroidized perlite in zone 1 are oriented along the lines of deformation localization, the thickness of which is $\sim 5-10\,\mu$m.

Ansys Autodyn software package was used for selection of constants. It was applied for simulation of collision of

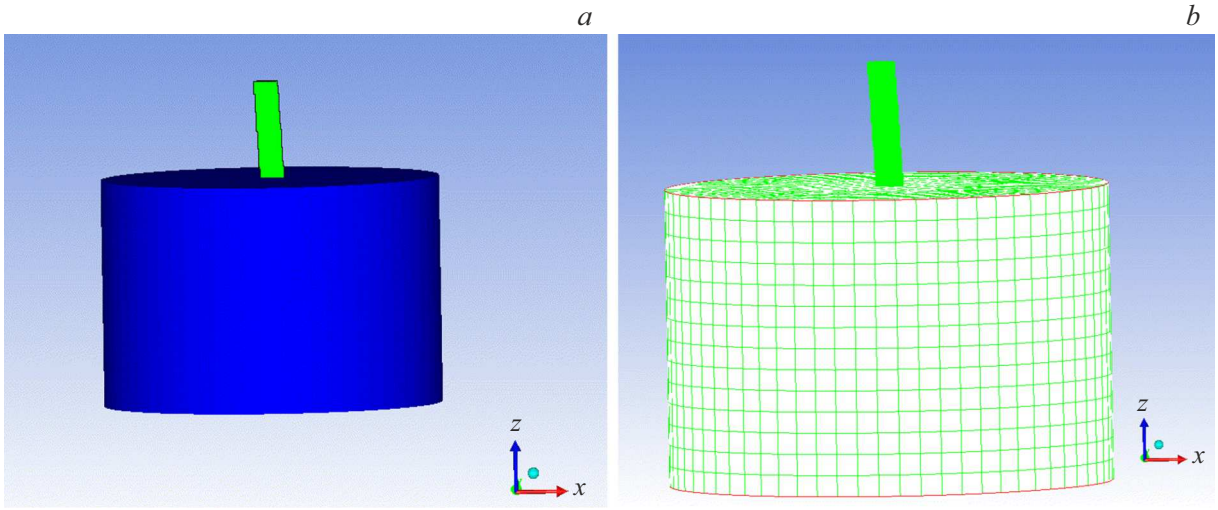

Fig. P3. Geometry of the system in modeling of explosive hardening (*a*). A finite element grid (barrier) and a system of SPH particles (sample) (*b*).

5×25 mm samples and 90×60 mm steel barrier (Fig. P3, *a*). The characteristics of the Structural Steel material from the ANSYS material database were used for simulation of the barrier material. Fig. P3, *b* shows the finite element grid used for solving the problem.

The geometric parameters of the model object and the steel sample were compared after a collision with a flat barrier to determine the parameters of the Johnson–Cook model (see equation (1)) for steel U8 (Fig. P1). The initial selection of constants of steel U8 was carried out based on the constants of the Steel 4340 material from the ANSYS material database. More than 300 combinations of constants have been tested. The optimal set of constants of steel U8 in the equation (1) was determined by comparing the simulation results with experimental data (Fig. P1): $A = 378$ MPa, $B = 664$ MPa, $n = 0.2$, $C = 0.07$, $m = 1.6$.

References

[1] V.K. Babich, Yu.P. Gul, I.E. Dolzhenkov. *Deformacionnoe starenie stali* (Metallurgiya, M., 320 p., 1972) (in Russian).
[2] C.C. Li, W.C. Leslie. Metall. Mater. Trans. A, **9**, 1765 (1978). DOI: 10.1007/BF02663406
[3] A. Karimi Taheri, T.M. Maccagno, J.J. Jonas. Mater. Sci. Technol., **11** (11), 1139 (1995). DOI: 10.1179/mst.1995.11.11.1139
[4] A.H. Cottrell, B.A. Bilby. Proc. Phys. Soc. Lond., **62** (1), 49 (1949). DOI: 10.1088/0370-1298/62/1/308
[5] A.P. Gulyaev. *Metallovedenie* (Metallurgiya, M., 647 p., 1977) (in Russian).
[6] T. Teshima, M. Kosaka, K. Ushioda, N. Koga, N. Nakada. Mater. Sci. Eng. A, **679**, 223 (2017). DOI: 10.1016/j.msea.2016.10.018
[7] H. Zheng, L. Fu, X. Ji, Y. Ding, W. Wang, M. Wen, A. Shan. Mater. Sci. Eng. A, **824**, 141860 (2021). DOI: 10.1016/j.msea.2021.141860
[8] Yu.F. Ivanov, A.A. Yuryev, V.E. Gromov, S.V. Konovalov, O.A. Peregudov. Izv. vuz Chern. metal., **61** (2), 140 (2018) (in Russian). DOI: 10.17073/0368-0797-2018-2-140-148
[9] D.A. Porter, K.E. Easterling, G.D.W. Smith. Acta Metall., **26** (9), 1405 (1978). DOI: 10.1016/0001-6160(78)90156-6
[10] V.I. Izotov, V.A. Pozdnyakov, E.V. Lukyanenko, O.Yu. Usanova, G.A. Filippov. FMM, **103** (5), 549 (2007) (in Russian).
[11] Y. Zhao, Y. Tan, X. Ji, Z. Xiang, Y. He, S. Xiang. Mater. Sci. Eng. A, **731**, 93 (2018). DOI: 10.1016/j.msea.2018.05.114
[12] Vl.Vl. Balandin. PPP, **75** (3), 232 (2013) (in Russian). DOI: 10.32326/1814-9146-2013-75-3-232-237
[13] V.V. Balandin, V.V. Balandin, A.M. Bragov, V.L. Kotov. Tech. Phys., **61** (6), 860 (2016). DOI: 10.1134/S1063784216060037
[14] M.S. Blunter, Yu.V. Piguzov, G.M. Ashmarin and others. *Metod vnutrennego treniya v metallovedcheskikh issledovaniyakh* (Metallurgiya, M., 1991), 248 p. (in Russian).
[15] I.S. Golovin. *Neuprugost', vnutrennee trenie i mekhanicheskaya spektroskopiya metallicheskikh materialov* (MISIS, M., 2020), 247 p. (in Russian).
[16] A. Novik, B. Berry. *Relaksacionnye yavleniya v kristallakh.* Translated from English, edited by E.M. Nagorny, Ya.M. Soifer (Atomizdat, M., 1975), 472 p. (in Russian).
[17] G.R. Johnson, W.H. Cook. Eng. Fract. Mech., **21** (1), 31 (1983).
[18] G.I. Taylor. Proc. R. Soc. Lond., **194** (1038), 289 (1948). DOI: 10.1098/rspa.1948.0081
[19] V.M. Shchastyantsev, D.A. Mirzaev, I.L. Yakovleva, K.Yu. Okishev, T.I. Tabatchikova, Yu.V. Khlebnikova. *Perlit v uglerodistykh stalyakh* (Yekaterinburg, Ural Branch of the Russian Academy of Sciences, 2006) (in Russian).
[20] K.V. Popov. *Dinamicheskoe deformacionnoe starenie metallov i khrupkost' vodorodnogo tipa* (Nauka, Novosibirsk, 1969), 96 p. (in Russian).
[21] W.S. Lee, C.F. Lin. Mater. Sci. Eng. A, **308** (1–2), 124 (2001). DOI: 10.1016/S0921-5093(00)02024-4
[22] P. Lisiecka-Graca, K. Bzowski, J. Majta, K. Muszka. Archiv. Civ. Mech. Eng., **21**, 84 (2021). DOI: 10.1007/s43452-021-00239-x

[23] N.N. Davidenkov, S.E. Belyaev, M.P. Markovets. Zav. lab., **21** (10), 964 (1945) (in Russian).
[24] G.I. Kanel, S.V. Razorenov, A.V. Utkin, V.E. Forts. *Eksperimental'nye profili udarnykh voln v kondensirovannykh sredakh* (Fizmatlit, M., 2008), 245 p. (in Russian).
[25] G.N. Epstein. *Stroenie metallov, deformirovannykh vzryvom* (Metallurgiya, M., 1988), 280 p. (in Russian).
[26] U. Andrade, M.A. Meyers, K.S. Vecchio, A.H. Chokshi. Acta Metal. Mater., **42** (9), 3183 (1994). DOI: 10.1016/0956-7151(94)90417-0

Translated by A.Akhtyamov